

Short Note

Simple factorization of implicit finite-difference downward-continuation operators

Biondo Biondi¹

INTRODUCTION

Solving the one-way wave equation by using implicit finite-differences on helical boundary conditions is a computationally attractive way to avoid the operator anisotropy induced by splitting (Rickett et al., 1998; Rickett, 2000). The method relies on a numerical spectral factorization of a finite-difference operator into the product of two operators: one minimum phase and the other maximum phase. When the velocity is laterally constant this factorization can be efficiently and reliably performed in the Fourier domain using the Kolmogoroff method (Claerbout, 1976). Unfortunately, when the velocity is laterally varying the operator to be factored is non-stationary, and Kolmogoroff cannot be directly applied. Rickett describes an approximate method to address this problem (2000), but unfortunately when the velocity field is rapidly changing instability may incur.

I attempt to circumvent the problems of factoring a non-stationary operator by analytical approximating the finite-difference operator as the cascade of operators that are either causal or anti-causal. The application of such one-sided operators by implicit finite-difference (e.g. Crank-Nicolson) requires only the inversion of triangular matrices, which is quickly accomplished by back substitution (i.e. polynomial division).

I am interested to achieve wide-angle accuracy, thus I concentrate my attention on the finite-difference step of the Fourier-Finite Difference Plus Interpolation (FFDPI) method that I previously presented (2000), which, in turn, is based on the Fourier-Finite Difference (FFD) method introduced by Ristow and Ruhl (1994).

The FFDPI correction term can be written in matrix notation as

$$\exp(\Delta k_z) = \exp\left(\Delta \frac{\Sigma' D' D \Sigma}{I - \Sigma' D' D \Sigma}\right), \quad (1)$$

where Δ and Σ are diagonal matrices function of the reference velocity and the true medium velocity, and $D' D$ is a discrete approximation of the Laplacian. The goal is to approximate Δk_z as the sum of terms that are function of only either D or D' . Since Δk_z is an exponent, the

¹email: biondo@sep.stanford.edu

approximation by a sum is equivalent to applying the corresponding implicit finite-difference operators in a cascade.

If we consider the simplest case of a two terms approximation we have

$$\Delta k_z \approx \Delta k_z^- (D') + \Delta k_z^+ (D). \quad (2)$$

The above sum would not require any approximation if D were symmetric; that is, its Fourier-domain representation were purely real. However, such factorization of the Laplacian would not be useful for our purposes, because it would not generate a triangular linear system when applied to an implicit finite-difference scheme.

Zhang et al. (2000) use a cascade similar to equation (2) together with helical boundary conditions to derive an efficient implicit finite-difference method that solves the two-dimensional one-way wave equation along the Cartesian axes and the diagonals. My goal is to employ the cascade in equation (2) together with helical boundary conditions to solve directly the three-dimensional problem, in a way similar to Rickett et al (1998). However, this note is limited to the analysis of the inaccuracies introduced by the factorization when solving the two-dimensional one-way wave equation.

TWO SIMPLE APPROXIMATIONS

I will consider the following two simple approximations:

$$\widehat{\Delta k_z} = -\frac{\Delta \Sigma' D'}{2(I + \Sigma' D')} + \frac{\Delta D \Sigma}{2(I - D \Sigma)} \quad (3)$$

and

$$\widetilde{\Delta k_z} = \frac{\Delta \Sigma' D'}{2(I + \Sigma' D')} + \frac{\Delta D \Sigma}{2(I + D \Sigma)}. \quad (4)$$

If the coefficients of Δ and Σ are constant; i.e., the reference velocity and the medium velocity are laterally invariant, the analysis can be performed in the wavenumber domain (k). In the following, I will assume that the operators are in the wavenumber-domain. It is straightforward to verify that

$$\widehat{\Delta k_z} = \Delta k_z \text{ if } \Im(D) = 0. \quad (5)$$

However, as discussed above, we want to use minimum-phase approximations of D . Minimum phase functions are by definition one sided, and thus the imaginary part of their wavenumber-domain representation must be different from zero. When this occurs, both a phase error $[\Re(\Delta k_z - \widehat{\Delta k_z})]$ and an amplitude error $[\Im(\widehat{\Delta k_z})]$ are introduced. The amplitude error is particularly troubling because it may cause either instability or excessive dumping of the propagating waves, depending on the sign of $\Im(\widehat{\Delta k_z})$.

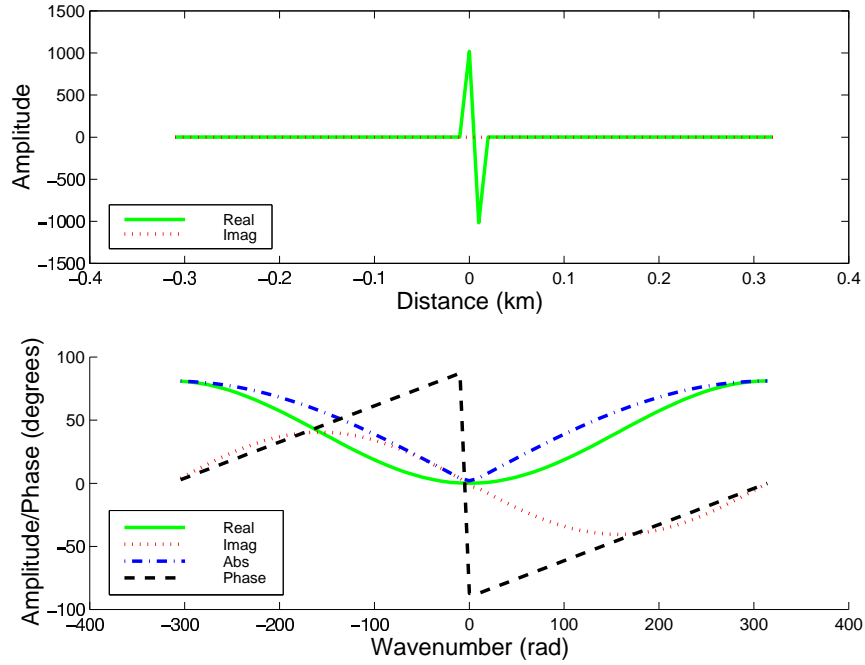


Figure 1: First-order approximation of the one-dimensional gradient operator. Notice that this operator is also minimum phase. Space-domain representation (top), wavenumber-domain representation (bottom). `biondo1-rep1` [CR]

In contrast, it is also easy to verify that

$$\Im(\widetilde{\Delta k_z}) = \Im(\Delta k_z) = 0 \text{ if } D(k) = D^*(-k); \quad (6)$$

that is, if the space-domain representation of D is purely real. This property of equation (4) is attractive because it means that the all-pass properties of $\exp(\Delta k_z)$ are preserved.

The analytical expressions of the errors introduced by the above approximations are not particularly insightful. Therefore, I will show the errors introduced by the approximations for some concrete instances of both D and the velocities. In particular, I will show the effective phase curves corresponding to the use of each approximation and compare them with the phase curves corresponding to the application of the exact FFD correction [equation (1)], and the application of a simple split-step correction.

I start by using for D the first-order approximation of the derivative operator. Figure 1 shows the space-domain representation (top), and the wavenumber-domain representation (bottom), of D . Notice that $D \Im(D) \neq 0$. D is also minimum phase.

Figure 2 shows the phase curves plotted as a function of the propagation angle. The approximate FFD curves correspond to the approximation of equation (3). The phase curves were computed assuming a medium velocity of 2 km/s, a low reference velocity of 1.7 km/s, a high reference velocity of 2.3 km/s, a spatial sampling rate of 10 m, and a temporal frequency of 25 Hz. Figure 3 shows the phase curves computed with the same parameters as in Figure 2,

with the exception of the temporal frequency, that was set to 100 Hz. The phase curves are affected by the temporal frequency for two reasons: first, $\Im(D)$ is function of the wavenumber (bottom of Figure 1); second, the higher the temporal frequency, the worse D'/D approximates the Laplacian, affecting the accuracy of the “exact” FFD correction. The frequency of 100 Hz corresponds to the Nyquist wavenumber for the waves propagating at 90 degrees with velocity of 2 km/s. From Figure 2 we can immediately conclude that $\widehat{\Delta k_z}$ is a poor approximation at low frequencies, even worse than the simple split-step correction. The curves corresponding to Δk_z and $\widehat{\Delta k_z}$ get closer at higher frequencies, but mostly because Δk_z becomes more ineffective. The phase errors for $\widehat{\Delta k_z}$ are sufficiently discouraging that I do not show the amplitude curves; that are related to the imaginary part of $\widehat{\Delta k_z}$.

In contrast, the approximation of equation (4) is more promising, not only because of its lack of stability problems [equation (6)], but because the phase errors are better behaved. Figures 4 and 5 show the phase curves corresponding to $\widetilde{\Delta k_z}$. At low frequency (25 Hz) the approximate FFD correction is worse than the exact one, but is better than the simple split-step correction (Figure 2). At high frequency (100 Hz), the approximate FFD correction is very close to the exact one (Figure 5).

The final goal is to solve the 3-D one-wave equation, not the 2-D one. The 2-D Laplacian cannot be as easily factored analytically as the 1-D one, and thus I would need to rely to numerical methods to find appropriate expressions for D . In particular, I would need to apply Kolmogoroff factorization. Figures 6 and 7 show the step of such procedure for the 1-D case. Figure 6 shows the zero-phase first derivative operator obtained by inverse Fourier transforming $D(k) = |k|$. Figure 7 shows the result of Kolmogoroff applied to the operator in Figure 6. Notice the similarity with the operator shown in Figure 1. The small wiggles following the large negative spike in the space-domain representation shown in Figure 7 are responsible for the difference in behavior at high wavenumbers. The phase curves for this choice of D are shown in Figures 8 and 9. They are very similar to the ones shown in Figures 4 and 5, with the exception of the curves corresponding to the “exact” FFD correction. Because the new D is a better approximation of the derivative operator also for high wavenumber, the curves corresponding to 100 Hz are almost identical to the ones corresponding to 25 Hz.

CONCLUSIONS

The problems encountered when factoring a non-stationary operator for applying the FFD correction with laterally varying velocity can be circumvented by approximating the exact FFD correction as the sum of terms that contains either causal or anti-causal operators.

The first approximation that I considered is unattractive both because of its phase errors and because of its potential for instability. The second approximation that I analyzed has the desired amplitude behavior and better phase properties than the first one. However, its usefulness is still undetermined by the results obtained so far. The errors introduced by these approximations should be weighted against the errors introduced by splitting, also taking into account that the splitting errors are greatly reduced in the FFDPI algorithm (Biondi, 2000), with respect to the simple FFD algorithm.

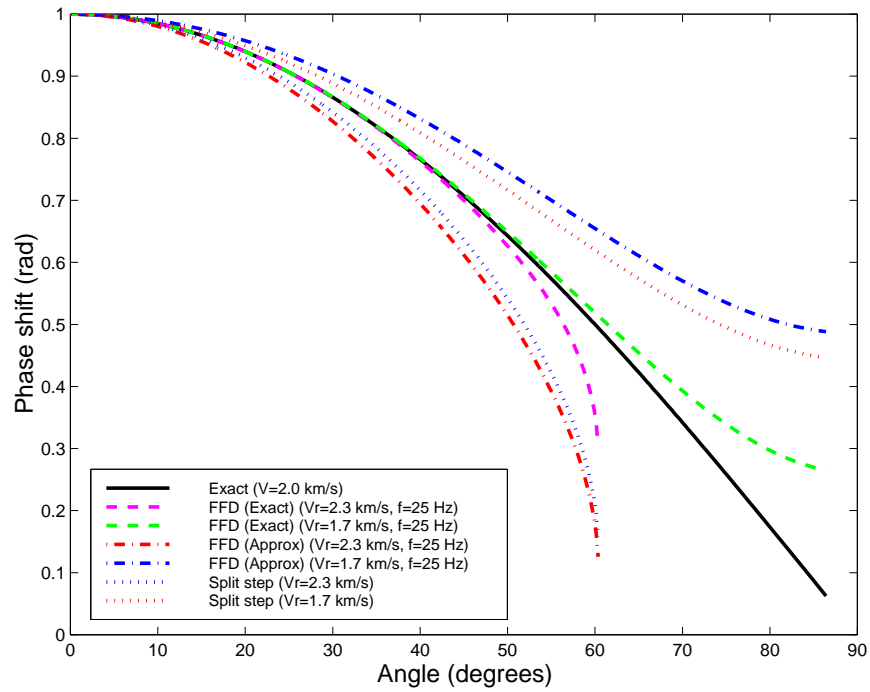


Figure 2: Phase curves obtained using the D operator shown in Figure 1, and for a temporal frequency of 25 Hz. The phase curves for the approximate FFD correction were computed using the approximation in equation (3). [biondo1-firsta1f25](#) [CR]

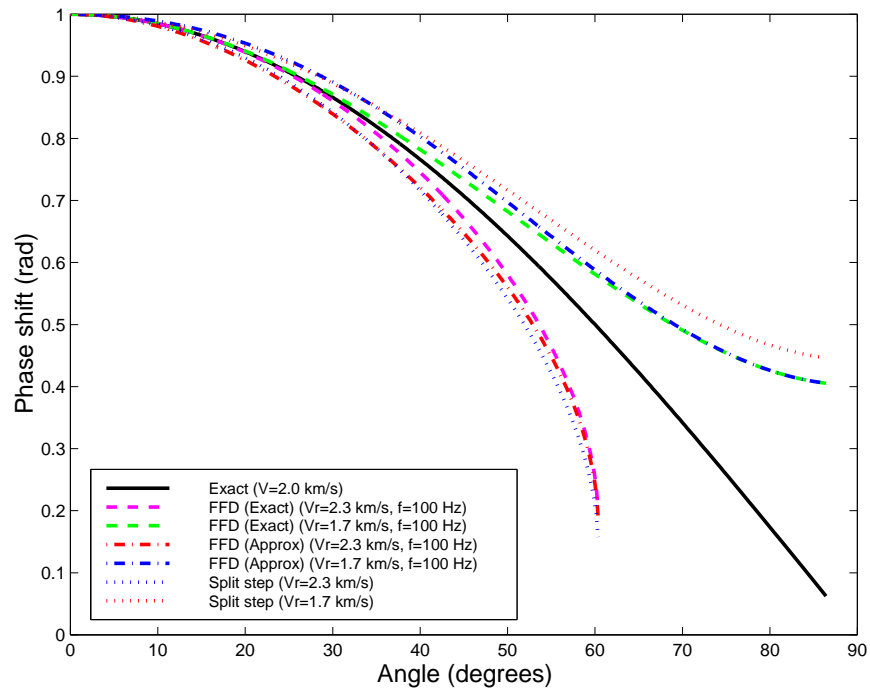


Figure 3: Phase curves obtained using the D operator shown in Figure 1, and for a temporal frequency of 100 Hz. The phase curves for the approximate FFD correction were computed using the approximation in equation (3). [biondo1-firsta1f100](#) [CR]

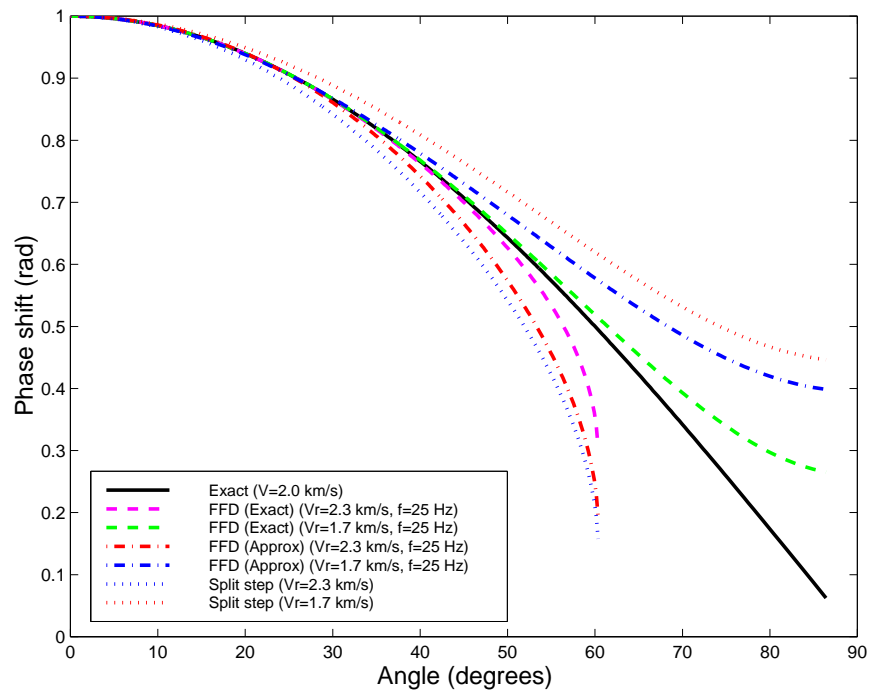


Figure 4: Phase curves obtained using the D operator shown in Figure 1, and for a temporal frequency of 25 Hz. The phase curves for the approximate FFD correction were computed using the approximation in equation (4). [biondo1-firsta2f25](#) [CR]

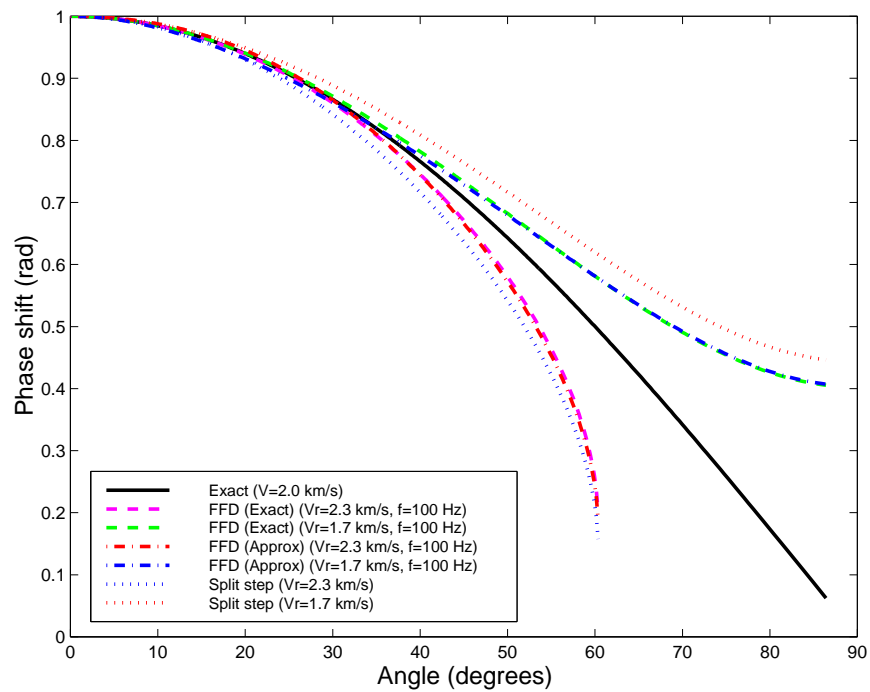


Figure 5: Phase curves obtained using the D operator shown in Figure 1, and for a temporal frequency of 100 Hz. The phase curves for the approximate FFD correction were computed using the approximation in equation (4). [biondo1-firsta2f100](#) [CR]

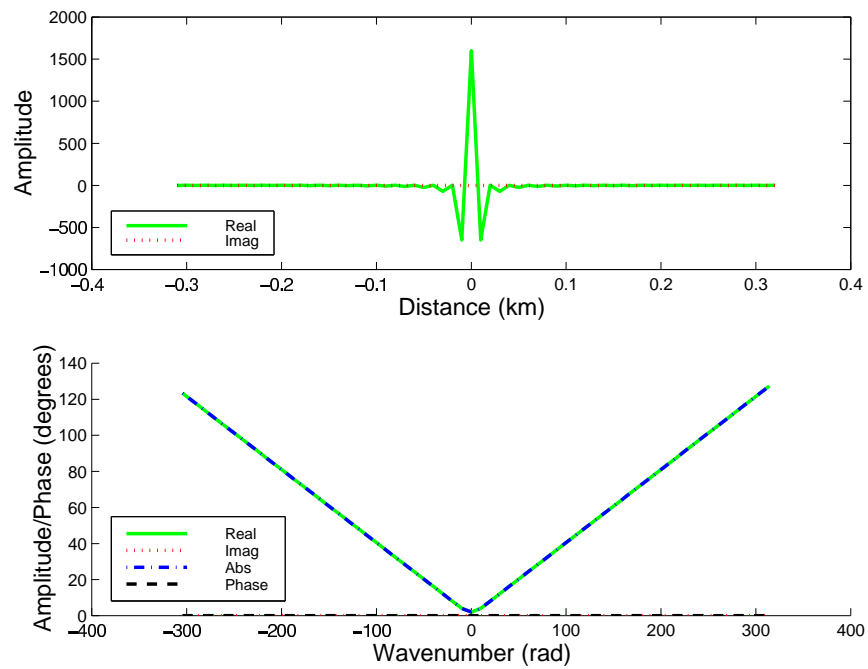


Figure 6: Zero-phase version of the exact one-dimensional gradient operator. Space-domain representation (top), wavenumber-domain representation (bottom). Notice that the imaginary part of the wavenumber-domain representation is equal to zero. [biondo1-rep2](#) [CR]

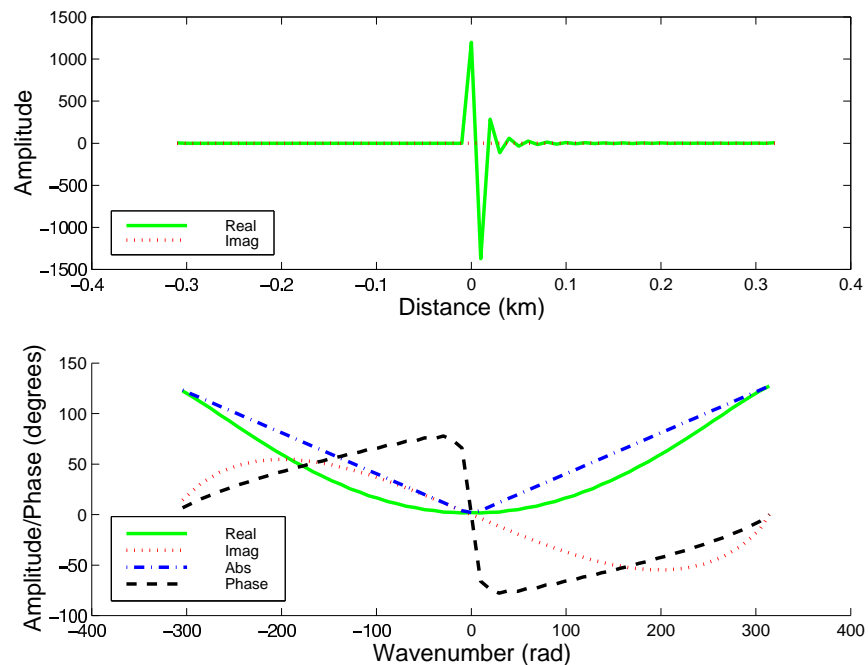


Figure 7: Minimum-phase version of the exact one-dimensional gradient operator. Space-domain representation (top), wavenumber-domain representation (bottom). Notice that the imaginary part of the wavenumber-domain representation is different from zero. [biondo1-rep3](#) [CR]

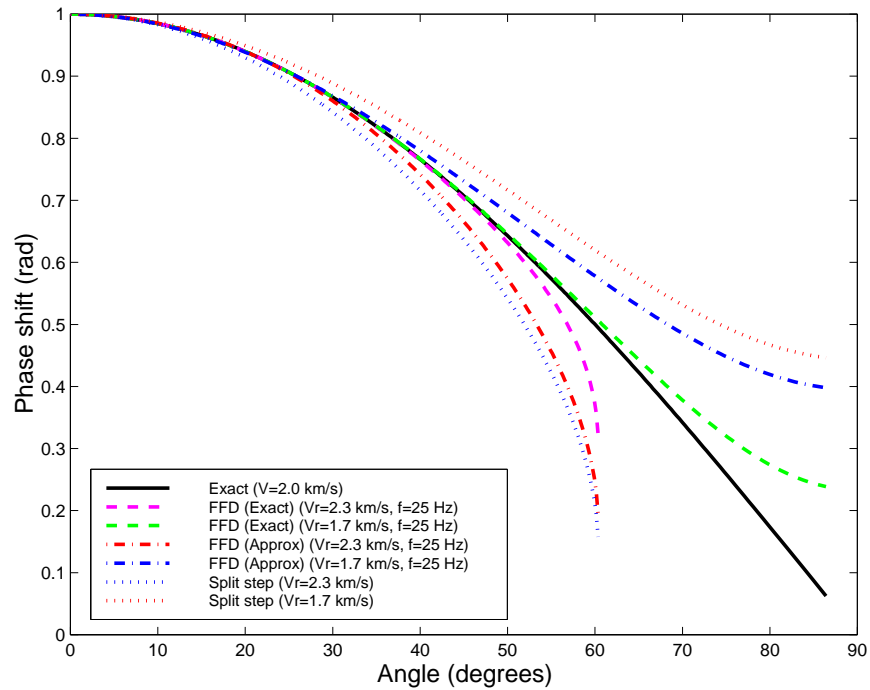


Figure 8: Phase curves obtained using the D operator shown in Figure 7, and for a temporal frequency of 25 Hz. The phase curves for the approximate FFD correction were computed using the approximation in equation (4). [biondo1-dera2f25](#) [CR]

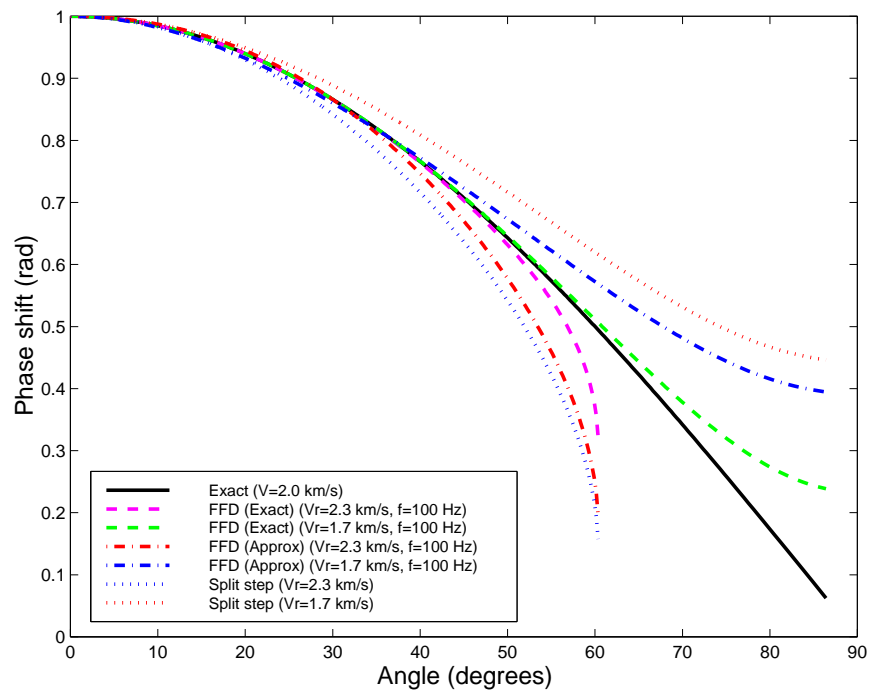


Figure 9: Phase curves obtained using the D operator shown in Figure 7, and for a temporal frequency of 100 Hz. The phase curves for the approximate FFD correction were computed using the approximation in equation (4). [biondo1-dera2f100](#) [CR]

REFERENCES

- Biondi, B., 2000, Stable wide-angle Fourier-finite difference downward extrapolation of 3-D wavefields: *SEP-103*, 79–103.
- Claerbout, J. F., 1976, *Fundamentals of Geophysical Data Processing*: Blackwell Scientific Publications.
- Rickett, J., Claerbout, J., and Fomel, S., 1998, Implicit 3-D depth migration by wavefield extrapolation with helical boundary conditions: 68th Ann. Internat. Meeting, Soc. Expl. Geophys., 1124–1127.
- Rickett, J., 2000, Efficient 3-D wavefield extrapolation with Fourier finite-differences and helical boundary conditions: *SEP-103*, 103–109.
- Ristow, D., and Ruhl, T., 1994, Fourier finite-difference migration: *Geophysics*, **59**, no. 12, 1882–1893.
- Zhang, G., Zhang, Y., and Zhou, H., 2000, Helical finite-difference schemes for 3-D depth migration: 70th Ann. Internat. Meeting, Soc. Expl. Geophys., accepted for publication.

